Science of the Total Environment 776 (2021) 146027

Contents lists available at ScienceDirect

Science of the Total Environment

journal homepage: www.elsevier.com/locate/scitotenv

Spatiotemporal changes in global nitrogen dioxide emission due to COVID-19 mitigation policies

Qian Liu [a], Anusha Srirenganathan Malarvizhi [a], Wei Liu [a], Hui Xu [b], Jackson T. Harris [c], Jingchao Yang [a], Daniel Q. Duffy [d], Michael M. Little [d], Dexuan Sha [a], Hai Lan [a], Chaowei Yang [a,*]

[a] NSF Spatiotemporal Innovation Center, George Mason Univ., Fairfax, VA 22030, USA
[b] Earth System Science Interdisciplinary Research Center, University of Maryland at College Park, College Park, MD 20740, USA
[c] Department of Geography, Dartmouth College, Hanover, NH, 03755, USA
[d] NASA Goddard, Computational and Information Sciences and Technology Office, Greenbelt, MD 20771, USA

HIGHLIGHTS

- The impacts of COVID-19-related interventional policies on NO_2 emissions are analyzed over different countries.
- The lockdown policy reduced the overall trend of NO_2 emissions in most target countries.
- Detrending analysis is conducted to mitigate the influences of inter-annual trends.
- After reopening, trends of national-mean NO_2 emissions returned to normal track in most target countries.

GRAPHICAL ABSTRACT

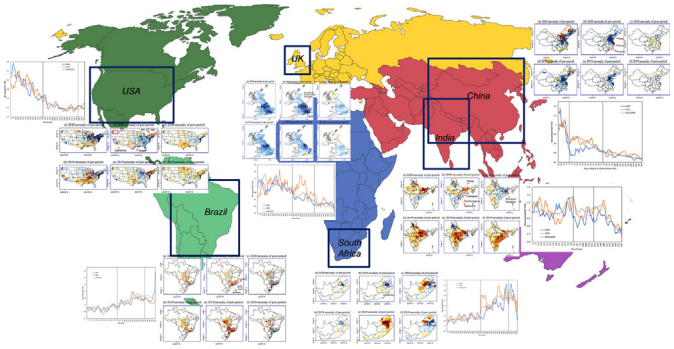

ARTICLE INFO

Article history:
Received 20 December 2020
Received in revised form 8 February 2021
Accepted 18 February 2021
Available online 22 February 2021

Editor: Jay Gan

Keywords:
COVID-19
Nitrogen dioxide
Lockdown
Relative difference
Spatiotemporal analysis

ABSTRACT

This paper investigates spatiotemporal changes of nitrogen dioxide (NO_2) tropospheric vertical column density due to the COVID-19 pandemic using satellite observations before, during and after the lockdown (hereafter referred as the pre-, peri- and post-periods) in six different countries: China, South Africa, Brazil, India, the UK and the US, and compare these periods with 2019 as well as mean climatology from 2010 to 2019. We observe significant declines in relative differences (RDs) from the pre- to peri-period (as compared with the 10-year climatology) in most study countries including China, South Africa, India, and the UK by 15, 17, 8 and 7% respectively. The US does not demonstrate significant decline with RD difference relatively small at just 2%. Meanwhile, although the 2020 RD of Brazil is 7% lower than 2010–2019, this trend is quite similar to that of 2019 (20% vs 23%). In the post-period of 2020, the NO_2 columns rebound in most target countries: China, US, South Africa, Brazil and UK, with similar RDs relative to the corresponding pre-period as compared with 2019 and 2010–2019. In contrast, NO in India continues to be influenced by the ongoing COVID-19 crisis with pre-to-post RD 8% lower than the average of previous 10 years.

1. Introduction

The 2019 coronavirus pandemic (COVID-19) has lasted one whole year, tremendously impacting economies, the environment, and people's daily lives on a global scale (Yang et al., 2020; Liu et al., 2020a, 2020b, 2020c, 2020d; Zambrano-Monserrate et al., 2020). Mitigation policies intended to reduce the spread of the virus – such as city lockdowns, social

* Corresponding author at: NSF Spatiotemporal Innovation Center/George Mason University, 4400 University Dr., Exploratory Hall, Room 2211, Fairfax, VA 22030, USA.
E-mail address: cyang3@gmu.edu (C. Yang).

https://doi.org/10.1016/j.scitotenv.2021.146027
0048-9697/

distancing, reduction of transportation and commuting, and shutdowns of non-essential industries–have been established in almost every country. With initial control of the COVID-19 pandemic in many countries, reopening has been put at the forefront of government agendas globally.

Nitrogen oxide (NO_x), the sum of nitric oxide (NO) and nitrogen dioxide (NO_2), plays an essential role in the composition of the earth's atmosphere (Crutzen, 1979) and has great effects on the earth's surface environment (Judeikis and Wren, 1978). It is one of the most crucial indicators of air quality over urban and industrial centers due to its importance in the catalytic production of the earth's ozone distribution (Villena et al., 2012) and formation of secondary inorganic aerosols (Behera and Sharma, 2011), with vital consequences for the global climate (Brinksma et al., 2008) and human health (Atkinson et al., 2018). The primary sources of NO_x are anthropogenic fuel-combustions, especially from motor vehicle and industrial power plants (Richter et al., 2005). NO_2 is usually adopted as the indicator of larger group of NO_x which remains relatively close to emission sources due to its comparably short lifetime in the atmosphere, and therefore can be utilized to monitor both long- and short-term changes in fuel consumption (Duncan et al., 2016; Lee and Koutrakis, 2014; Liu et al., 2020a, 2020b, 2020c, 2020d). An accurate investigation and evaluation of the changes in NO_2 caused by COVID-19 over different countries is vital for global economic loss assessment, resource rearrangement and reopening strategy-planning. Furthermore, long-term exposure to NO_2 is considered to be one of the most important contributors to high fatality rates caused by COVID-19 (Ogen, 2020), and even short-term exposure may increase the risk of infection (Zu et al., 2020; Zhu et al., 2020). Therefore, analysis on the trends and patterns of NO_2 densities are also crucial for the understanding of COVID-19 spread and fatality.

Efforts have been made to address the impacts of COVID-19 mitigation policies on air quality and, by extension, human activities using NO_2 observations. Abrupt declines of NO_2 emissions were observed in many parts of the world during the pandemic (Liu et al., 2020c; Liu et al., 2020d; Baldasano, 2020; Otmani et al., 2020). Using satellite observations, Bauwens et al. (2020) found unprecedented NO_2 decreases over China, South Korea, western Europe, and the United States during the pandemic as compared with the same period in 2019. Liu et al. (2020c) found significant reduction of NO_2 columns over major power plants and roads with seasonal variations considered and excluded in the analysis of NO_2 patterns over California, USA. However, with the influence of climate change (Krotkov et al., 2016) and emission regulations over the past several years (Shou et al., 2020), inter-annual trends during the study period could introduce uncertainties and errors to the analysis and results. Furthermore, whether declines were due to COVID-19 mitigation policies or seasonal/periodical trends has rarely been addressed through previous studies. Liu et al. (2020d) utilized model simulations with constant NO_2 emissions before and during the lockdown to rule out the potential influences introduced by changes in meteorological conditions in the study over China and found that these influences are relatively small as compared with prolonged reductions. Whether the same conclusion can be found in other parts of the world is still up for debate. Furthermore, with city-reopenings implemented all over the world, whether NO_2 emissions have completely recovered to baseline levels still needs to be confirmed.

Previous studies have shown that the variations in NO_2 tropospheric vertical column densities (TVCDs) are generally consistent and reflect anthropogenic NOx emission variations (Li and Wang, 2019). This study utilizes spaceborne NO_2 TVCD observed by the Ozone Monitoring Instrument (OMI) aboard Aura satellite to analyze and compare the changes of NO_2 emissions before, during and after the 2020 COVID-19 lockdowns in China, the United States, South Africa, Brazil, India and UK with 2019 levels as well as the means of the same periods during 2010 to 2019 (hereafter referred to as 2010–2019). We compare the temporal trend of NO_2 TVCD in 2020 with both the preceding year, 2019, and long-term climatology trends (2010–2019) to conduct a comprehensive analysis examining whether the pandemic has caused extraordinary changes. Furthermore, when investigating the spatial patterns of the NO_2 TVCD changes due to COVID-19, the linear inter-annual trend of each pixel is ruled out by performing detrending analysis on 2020 data before comparing it with 2019 data to mitigate the possible influences of other factors such as climate change and emission regulation policies on NO_2 emission. We also adopt anomalies to cancel out the seasonal cycles and reveal a relative pure pattern caused by COVID-19.

The remainder of this paper is organized as follows: the study area, datasets and analysis methods are introduced in Section 2; the results are described in Section 3; further discussion is offered in Section 4; and conclusions are given in Section 5.

2. Material and methods

2.1. Study area and data

The study aims at investigating and comparing how NO_2 emission patterns were (are) influenced by COVID-19 mitigation policies all over the world. Therefore, the study countries were selected from different continents with varying COVID-19 spread rates and economic conditions. These countries include China, where the first cases were reported, the US, which has the largest confirmed case numbers in the world (Dong et al., 2020) at the time of writing (December 2020); Brazil and India, which are among the countries with top confirmed-case numbers; South Africa, which has the most confirmed cases on the African continent (Dong et al., 2020); the United Kingdom (UK), which has the most deaths due to COVID-19 in Europe at the time of writing (Dec. 2, 2020).

The Nitrogen Dioxide Product (OMNO2d) of the Ozone Monitoring Instrument (OMI) aboard NASA's Earth Observing System's (EOS) Aura satellite is used to analyze NO_2 TVCD in the pre-, peri- and post-period of target countries for both 2020 and 2010–2019. It is a level-3 gridded product where pixel-level data of good quality are binned and averaged into 0.25° global grids at a daily temporal resolution (Krotkov et al., 2016).

2.2. Analytical method

The study adopts the Government Response Stringency Index (GRSI, Hale et al., 2020), as shown in Fig. A.1, to generate lockdown and reopening dates corresponding to each target country. Lockdown dates are selected when the GRSI rises above 70, while reopening dates are elected when the stringencies significantly decline from the GRSI peak. Note that there is no arbitrary threshold selected for the reopening dates because mitigation policies differ across countries; these dates reflect the major conditions of those countries, but some cities and industries may have already been shut down or reopened before the dates. Table 1 presents detailed shutdown and reopening dates of target countries. The study adopts day-of-year for all the dates in order to avoid the leap year issue in the calculation of long-term climatology.

Analysis for China is based on lunar dates because the outbreak period overlapped with Chinese New Year (CNY) which has critical influence on NO_2 emission due to national holidays (Jie et al., 2016). The start dates of the study are 20 days before CNY for China and January 1 for all the other countries; the end date is 165 days after CNY for China and June 30 for others.

Table 1
Shutdown and reopening dates in study countries, numbers in the brackets indicates the day-of-year of these dates.

Country	Shutdown start date	Reopening start date
China	01/25/2020 (1 in lunar calendar)	04/09/2020 (77 in lunar calendar)
USA	03/21/2020 (81)	06/14/2020 (166)
South Africa	03/26/2020 (87)	06/07/2020 (159)
Brazil	03/21/2020 (81)	06/01/2020 (153)
India	03/24/2020 (84)	05/04/2020 (125)
UK	03/22/2020 (82)	05/14/2020 (135)

The USA was struck by large wildfires starting in May 2020 with approximately 2.2 million more acres burned than the 10-year average and almost double the acreage burned in the 2019 season as of Nov. 10 (CDP, 2020). In order to avoid the influence of wildfires, the end of peri-period for the USA is set as April 30.

We calculate the climatology of global NO_2 TVCD and pixels with annual means smaller than 1×10^{15} molec/cm^2 are not considered to be dominated by anthropogenic sources, thus are not included in the whole procedure of spatiotemporal analytics.

2.2.1. Timeseries analysis

To investigate changes of spatial patterns in 2020 caused by COVID-19 related actions, the paper compares the NO_2 TVCD time series of 2020 with 2019. Through the comparison with long-term climatology and the adjacent year, annual patterns are removed in order to isolate changes potentially caused by COVID-19 mitigation measures. Detailed procedure is conducted through the following steps:

1) For each country, daily mean NO_2 TVCD is calculated by averaging all data in every day-of-year over the study period for 2019, 2020 and 2010–2019 using Eq. (1). Part of the single-pixel uncertainties of raw data will be canceled out by spatiotemporal averaging.

$$\overline{TVCD_t} = \frac{\sum_{i=1}^{m}\sum_{j=1}^{n} TVCD_{i,j,t}}{m\times n}, t = 1,2,3,\ldots,T_{study} \quad (1)$$

where t is the day-of-year, $\overline{TVCD_t}$ is the mean NO_2 TVCD on day t; (i, j) are the coordinates of the pixels; $m \times n$ is the number of available observations over this target country; T_{study} is the last day-of-year in the study period. For 2019 and 2020, all observations are averaged for each day throughout the study period. For 2010–2019, all available measurements from a specific day-of-year are averaged. Take day 1 as an example: day 1 observations of 2010, 2011, 2012, 2013, 2014, 2015, 2016, 2017, 2018 and 2019 are averaged as the daily mean value of day 1 in 2010–2019. So as for all other dates. Day-of-year is used instead of date due to the leap year issue.

2) The values generated from step 1 are normalized to the mean of their corresponding pre-period to make the trend of the three timeseries (2019, 2020 and 2010–2019) comparable using Eq. (2):

$$NTVCD_t = \frac{\overline{\mathrm{TVCD}_t}}{\overline{TVCD_{pre}}} \quad (2)$$

where $NTVCD_t$ is the normalized daily concentration of each air pollutant, $\overline{TVCD_{pre}}$ is the mean values of pre-periods in 2019, 2020 and 2010–2019 which is calculated based on Eq. (3):

$$\overline{TVCD_{pre}} = \frac{\sum_{t=1}^{n_{pre}} TVCD_t}{n_{pre}} \quad (3)$$

where n_{pre} is the number of days in the pre-period of each country.

3) Timeseries of the 7-day moving average are then calculated for 2019, 2020 and 2010–2019 to smooth out daily fluctuations.

2.2.2. Spatial analysis

Spatial patterns are analyzed as follows:

a) For each country, the periodical (pre-, peri- and post-period) mean TVCD of each covered pixel (i,j) are calculated for 2019 and 2020 using Eq. (4):

$$\overline{\mathrm{TVCD}}_{i,j} = \frac{\sum_{t=T_{period\ start}}^{T_{period\ end}} TVCD_{\mathrm{i,j,t}}}{T_{period}}, i\in m, j\in n \quad (4)$$

where t is the day-of-year, $\overline{\mathrm{TVCD}}_{i,j}$ is the mean NO_2 TVCD of the target period (pre-, peri- and post-period); (i, j) are the coordinates of the pixels; $m \times n$ is the number of available observations over this target country; $T_{period\ start}$ and $T_{period\ end}$ are the first and last day-of-year in the target period.

b) To rule out the potential influence of inter-annual trend between data of 2020 and 2019 on the spatial patterns, the study also performs detrending analysis on each pixel in the target countries for 2020 according to their specific ranges of the pre-, peri- and post-period respectively. Detrended TVCD of pixel (i, j), DTVCD $(2020)_{i,j}$, can be derived using Eq. (5):

$$\begin{aligned}\overline{DTVCD(2020)_{i,j}} &= \overline{TVCD(2020)_{i,j}} - a_{i,j} i\in m, j\in n\\ a_{i,j} &= slope(TVCD)2010\text{–}2019_{i,j}, x\end{aligned} \quad (5)$$

where $\overline{TVCD(2020)}_{i,j}$ is the mean TVCD of pixel (i,j) in 2020 during a specific period (pre, peri or post); $TVCD(2010-2019)_{i,j}$ encompasses every observation of the pixel during the target period in 2010–2019; x is an array containing consecutive integers from 1 to the total number of days in the period for the 10 years (2010–2019); $a_{i,j}$ is the inter-annual trend of pixel (i, j) which is also the slope of the linear regression between $TVCD(2010-2019)_{i,j}$ and x.

c) To further eliminate the influences of seasonal/periodical cycles among the pre-, peri- and post-period, for a specific period, we calculate the spatial distribution of anomalies by subtracting the 10-year climatology from the 2020 (detrended) and 2019 data for each pixel as shown in Eq. (6):

$$A_{i,j} = \overline{TVCD(i,j)}_{p,y} - \overline{TVCD(i,j)}_{p,2010-2019}, \mathrm{p}\in pre-, peri-and\ post-period, y = 2019, 2020 \quad (6)$$

where (i,j) is the coordinate of the pixel.

3. Results

Table 2 shows the overall relative differences (RDs) between the peri- and pre-period, and the post- and peri-period for 2020, 2019 and 2010–2019 in each country. RDs are calculated through Eq. (7):

$$RD = \frac{\overline{TVCD}_{period2} - \overline{TVCD}_{period1}}{\overline{TVCD}_{period1}} \times 100\% \quad (7)$$

where $\overline{TVCD}_{period2}$ and $\overline{TVCD}_{period1}$ are the average TVCD for the former and latter periods respectively in 2020, 2019 or 2010–2019. Major portions of the remaining systematic error will be canceled out by applying RD calculations (Bauwens et al., 2020).

Details are discussed in Sections 3.1 to 3.6.

3.1. China

The first few confirmed COVID-19 cases were reported in China's Wuhan city in December 2019. By the end of January 2020, all Chinese provinces initiated the highest response level to the public health emergency (Zu et al., 2020). In the pre-period, the daily time series of 2020 reveals a continuous decrease, reaching the minimum around January 25, the Chinese New Year (CNY), due to the gradual shutdown of industry prior to the country's biggest holiday, which is consistent with the data of 2019 and 2010–2019. A rebound is observed in the previous 10 years as well as 2019 around 1 week after CNY, when the holiday period ended. However, in 2020, the time-series does not display such a rapid uptick; NO_2 TVCDs stay at lower values until about 20 days after CNY and return to normal trends at a much slower rate as compared with 2019 and 2010–2019, 60 days after CNY when most cities and industries are gradually reopened in China. This low-emission period was

Table 2
Overall RD between the peri- and pre-period, and the post- and peri-period in different countries for 2020, 2019, and 2010–2019. Uncertainties within parentheses are the standard errors.

	Relative difference between peri- and pre-period (%)			Relative difference between post- and pre-period (%)		
	2020	2019	2010–2019	2020	2019	2010–2019
China	−53(±11)	−39(±8)	−38(±3)	−65(±11)	−62(±8)	−67(±3)
USA	−41(±5)	−40(±3)	−39(±2)	−48(±4)	−47(±3)	−53(±2)
South Africa	43(±6)	75(±8)	60(±3)	93(±12)	76(±10)	79(±4)
Brazil	20(±3)	23(±3)	27(±2)	27(±3)	23(±3)	36(±1)
India	−11(±3)	−1(±4)	−3(±1)	−14(±3)	−6(±3)	−6(±2)
UK	−34(±4)	−9(±7)	−27(±3)	−54(±4)	−46(±6)	−55(±2)

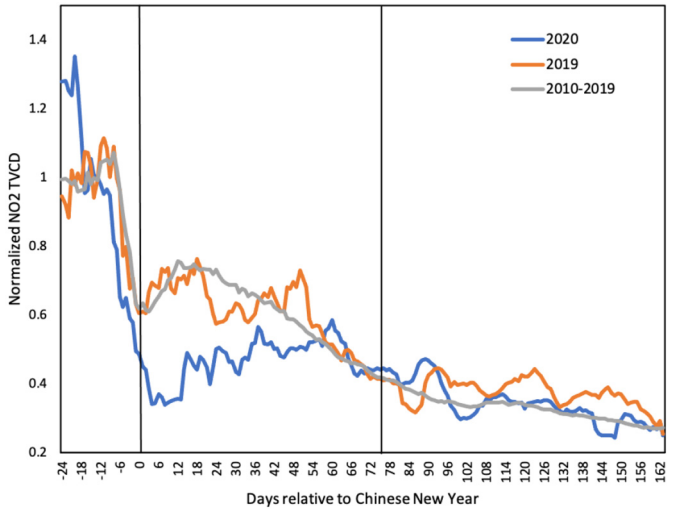

Fig. 1. Daily variations in 7-day moving averages of the NO_2 TVCD over China. The x-axis shows days relative to Chinese New Year. Points represent the midpoint of the 7-day interval. Values are normalized to the mean of the pre-period. The shadows represent standard errors. The two vertical lines divides the timeseries in to the pre-, peri- and post-periods.

prolonged for more than 40 days in 2020. As shown in Table 1, NO_2 TVCD declines by 53% through pre- to peri-period in 2020, which is far severer than in the same period of 2019 (−39%) and 2010–2019 (−38%); after reopening in 2020, the reduction of NO_2 columns show a similar level as compared with 2019 and 2010–2019 (−65% vs −62% and 67%), which indicates that the unusual decline was suppressed in 2020, potentially due to urban and industrial reopening. These results on time series analysis and overall statistics over China are consistent with the study of Liu et al. (2020d) (Fig. 1).

Fig. 2 shows NO_2 TVCD anomalies for pre-, peri- and post-period over China. We deem pixels with annual mean NO_2 TVCD smaller than 1×10^{15} molec/cm^2 as not dominated by anthropogenic sources, thus they are not plotted in all spatial results. In the pre-period, the 2020 data has higher values over most parts of China than 2019 (Fig. 2a and d), which rules out the possibility that 2020 has an initial lower NO_2 emission. However, during the peri-period of 2020, lower NO_2 TVCDs spreads to more surface area than in 2019. Wuhan city, where the first few confirmed cases were reported, shows an unprecedented low value in 2020 which cannot be observed in 2019. Other major cities such as Beijing and Guangzhou also present considerably lower TVCDs than previous year. These column reductions are likely due to the declines of traffic and vehicle use which is the dominate source of NO_2 emissions in cities.

The decreases in some industrial regions such as parts of Shanxi and Shandong province, where located large numbers of coal power plants (Boren, 2015; Fig. A.2), are potentially caused by the shutdown of non-essential industries and reducing of power plants' emissions.

In the post-period, columns in most parts of the southeastern and central China recover and even exceed the 2019 data. The observed increases are likely due to the recovery of industrial production and traffic emissions. However, the metropolises of Beijing and Wuhan still demonstrate lower emissions than usual, possibly due to the second outbreak in Beijing in June 2020 and more cautious reopening strategies in Wuhan.

3.2. USA

The first confirmed case in the US was reported on January 20, 2020 and 11 days later, the U.S. declared a public health emergency

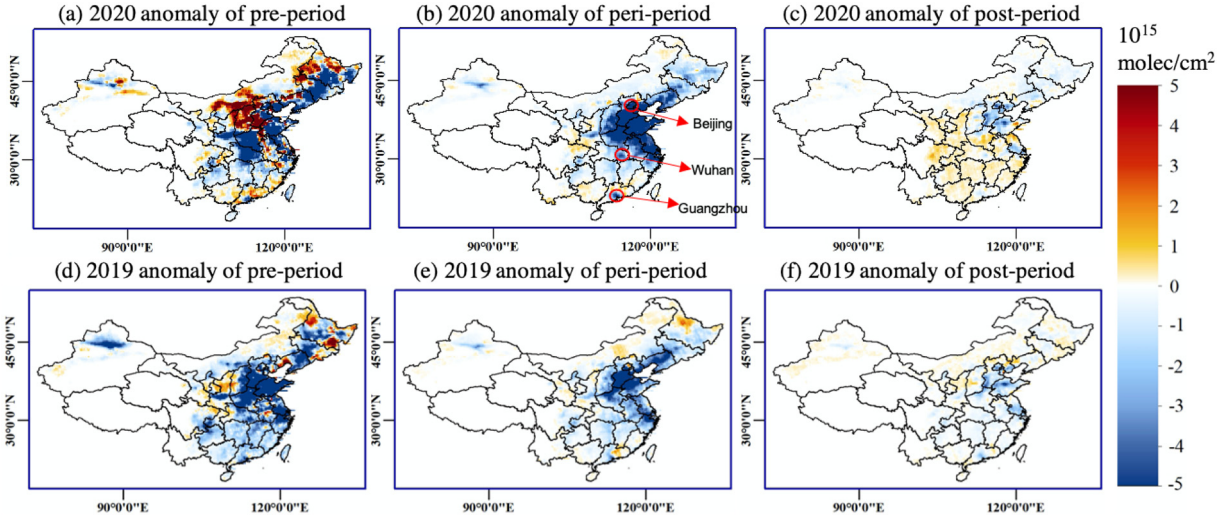

Fig. 2. Spatial patterns of NO_2 TVCD anomalies for pre-, peri- and post-period over China. (a)–(c) anomalies for 2019; (d)–(f) anomalies for 2020. Red circles are cities of Beijing, Wuhan and Guangzhou. Pixels with annual means smaller than 1×10^{15} molec/cm^2 are not plotted in the maps.

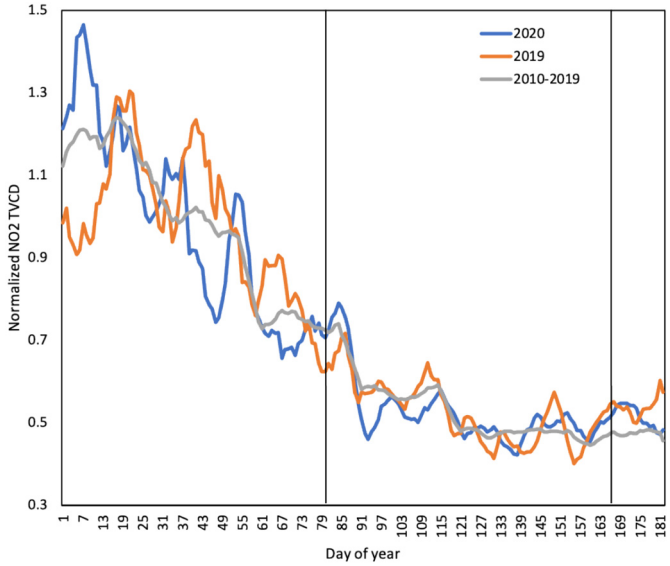

Fig. 3. Daily variations in 7-day moving averages of the NO_2 TVCD over USA. The x-axis shows day-of-year. Points represent the midpoint of the 7-day interval. Values are normalized to the mean of the pre-period. The shadows represent standard errors. The two vertical lines divides the timeseries into the pre-, peri- and post-period.

(Riechmann, 2020). Throughout March and early April, most state governments issued stay-at-home orders to stem the spread of the virus (Norwood, 2020). As shown in Fig. 3, the 2020 timeseries of daily NO_2 TVCD over the US is quite similar to that of 2019 and 2010–2019 from the pre- to peri-period; and the overall statistic listed in Table 2 also reveals similar reductions over these two periods in 2020, 2019 and 2010–2019 (−41%, −40% and −39% respectively) with differences smaller than the standard errors. After the reopening, an uptick in the timeseries of NO_2 columns can be observed for both 2020 and 2019, and the overall reductions are smaller in the recent years as compared to the 10-year climatology. In conclusion, COVID-19 related actions have not substantially influenced overall NO_2 emissions in the US.

According to Fig. 4, regions where the first COVID-19 breakouts occurred in the US, such as Washington state, California, New York and its neighboring states, Vermont and New Hampshire (Fig. 4b, red circles), show decreasing changes from the pre- to peri-period in 2020 as compared with 2019. In order to slow the spread, these states implemented mitigation policies including curfews, travel bans, transportation restrictions and industrial closures (Moon, 2020; McMichael et al., 2020). These declines are most likely due to the reduction of traffic emissions caused by these policies. Another NO_2 reduction evidence can be found along the national highway between Los Angeles and San Francisco. The anomalies are quite similar between 2020 and 2019 during pre-period, but obviously lower in 2020 during the peri-period. The reduction of traffic emission should account for this change. Eastern Texas also presents a decreasing trend which cannot be seen in 2019. This region is an industrial area concentrated with power plants (Fig. A.3). This reduction may largely be due to the closure of non-essential industries.

Aforementioned reasons also explain the declines over southeastern areas. However, regions circled in green in Fig. 4b show increasing changes during peri-period with extreme low values in the pre-period of 2020 compared to 2019. These significant positive changes counteract the declines and make the national average comparable with previous years.

After the economic reopening, NO_2 columns in most areas rebound and show similar values as 2019, indicating the recovery of industrial and traffic emissions. However, exceptions can still be found in the green-circled region, possibly due to low initial values in the pre-period.

3.3. South Africa

The first COVID-19 case in South Africa was reported on March 5, 2020 (South African Government, 2020a, 2020b). On March 26, 2020, a national lockdown was issued (Businesstech, 2020). As shown in Fig. 5, the trend of NO_2 columns in 2020 is generally lower than those of 2019 and 2010–2019 during peri-period especially for the first 20 days when the government announced a 21-day national lockdown. This coincidence indicates the influence of COVID-19 on industrial production and emission. The overall increase of NO_2 columns declines significantly in 2020 as compared with 2019 and 2010–2019 (43% vs 75% and 60%, Table 2) from the pre- to peri-period, reflecting an unusual reduction in NO_2 emissions. The increasing trend bounces back in the post-period with a RD of 93% compared with the pre-period, which is higher than both 2019 (76%) and 2010–2019 (79%). These patterns are due to the lockdown and reopening strategies established by the South African government to fight against COVID-19.

Through the results of the spatial analysis shown in Fig. 6, we notice that the significant decreases in NO_2 TVCDs from pre- to peri-period are mainly distributed over the city of Emalahleni, the legislative capital, Cape Town and the national boundary with Eswatini. These regions mostly showed increases in 2019. Transportation between the two countries was reduced due to the travel restriction announced by both

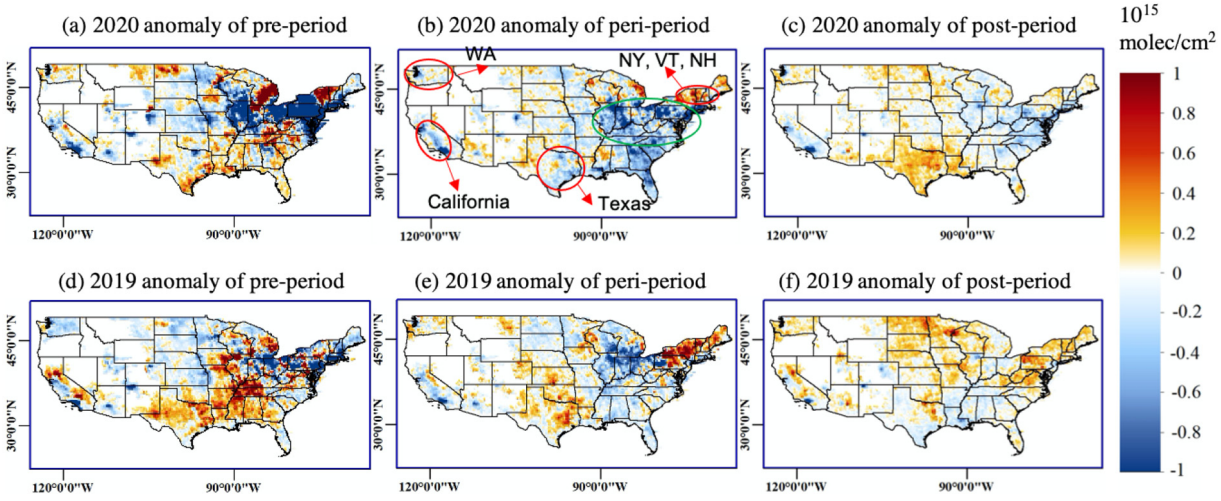

Fig. 4. Spatial patterns of NO_2 TVCD anomalies for pre-, peri- and post-period over the USA. (a)–(c) anomalies for 2019; (d)–(f) anomalies for 2020. Pixels with annual means smaller than 1×10^{15} molec/cm^2 are not plotted in the maps.

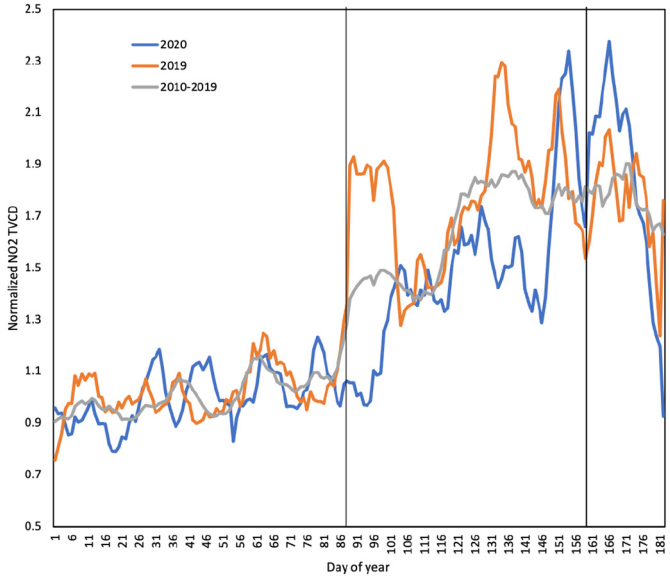

Fig. 5. Daily variations in 7-day moving averages of the NO_2 TVCD over South Africa. The x-axis shows day-of-year. Points represent the midpoint of the 7-day interval. Values are normalized to the mean of the pre-period. The shadows represent standard errors. The two vertical lines divides the timeseries in to the pre-, peri- and post-periods.

countries (South African Government, 2020b; The Government of the Kingdom of Eswatini, 2020). The declines in NO_2 TVCD may have a strong connection with these COVID-19 mitigation measures. Moreover, the decrease around Cape Town can also be explained by the traffic reduction under the country-wide lockdown order (Businesstech, 2020).

Furthermore, Emalahleni city and its surrounding regions is the most important coal-mining center of the country (Pollet et al., 2015; Fig. A.4), so the decreasing pattern also reflects the significant reduction of industry production in this area. After economic reopening, the spatial patterns of NO_2 TVCDs return to a similar level as the previous year for most areas, indicating that both industrial production and transportation have returned to normal levels.

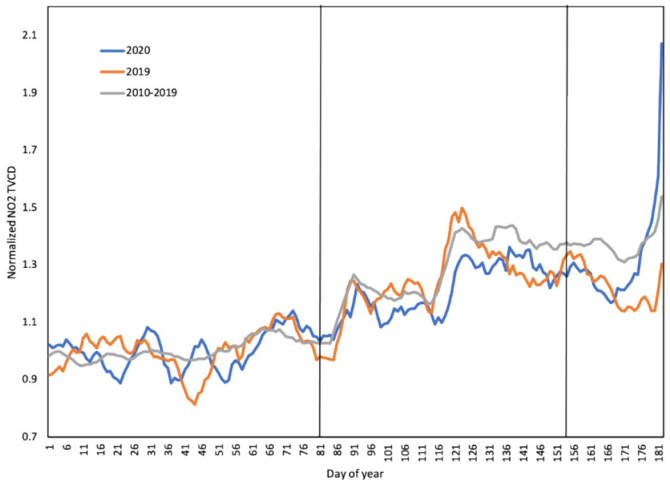

Fig. 7. Daily variations in 7-day moving averages of the NO_2 TVCD over Brazil. The x-axis shows day-of-year. Points represent the midpoint of the 7-day interval. Values are normalized to the mean of the pre-period. The shadows represent standard errors. The two vertical lines divides the timeseries in to pre-, peri- and post-periods.

3.4. Brazil

The COVID-19 virus was first confirmed in Brazil on February 25, 2020 (Ministerio da Saude, 2020) and had spread to every state in Brazil by March 21st (Charner, 2020). By the end of March, most state governments had imposed quarantine policies to slow the spread (BBC News, 2020). Fig. 7 shows the timeseries of normalized daily NO_2 TVCDs in 2020, 2019 and 2010–2019. The 2020 data shows a slight decrease as compared with 2019 and 2010–2019 during the lockdown (20% vs 23% and 27%). The trend of 2020 remains lower than the previous 10-years' climatology for a 20-day period after the end of lockdown.

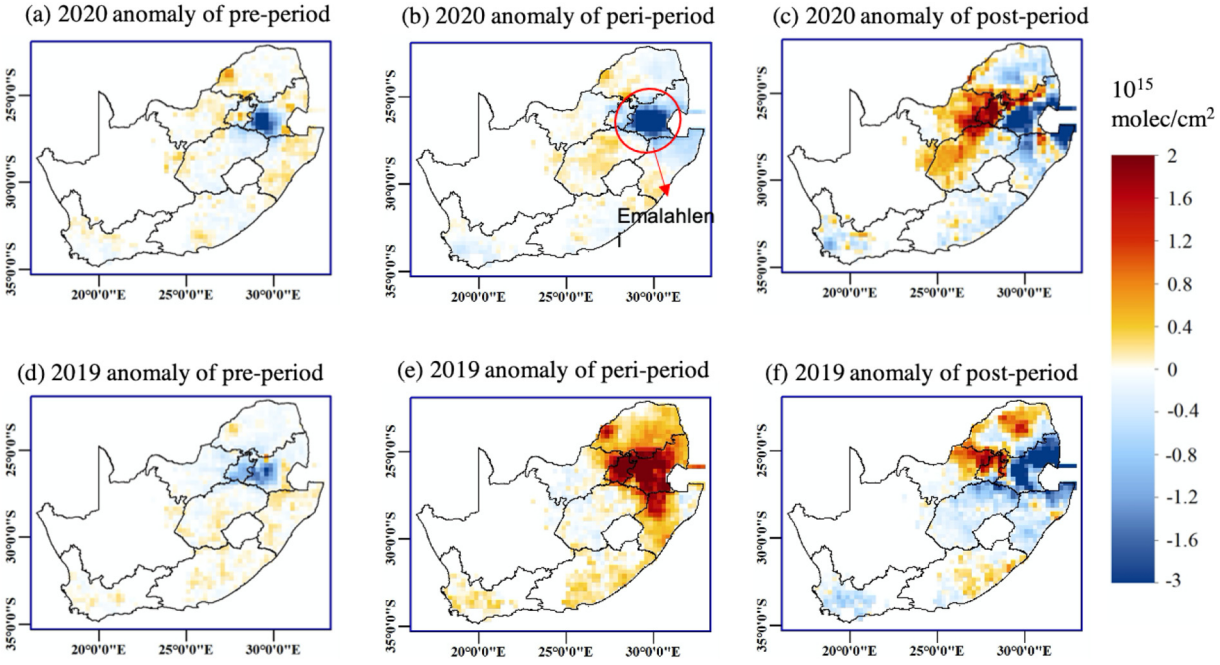

Fig. 6. Spatial patterns of NO_2 TVCD anomalies for pre-, peri- and post-period over South Africa. (a)–(c) anomalies for 2019; (d)–(f) anomalies for 2020. Pixels with annual means smaller than 1×10^{15} molec/cm^2 are not plotted in the maps.

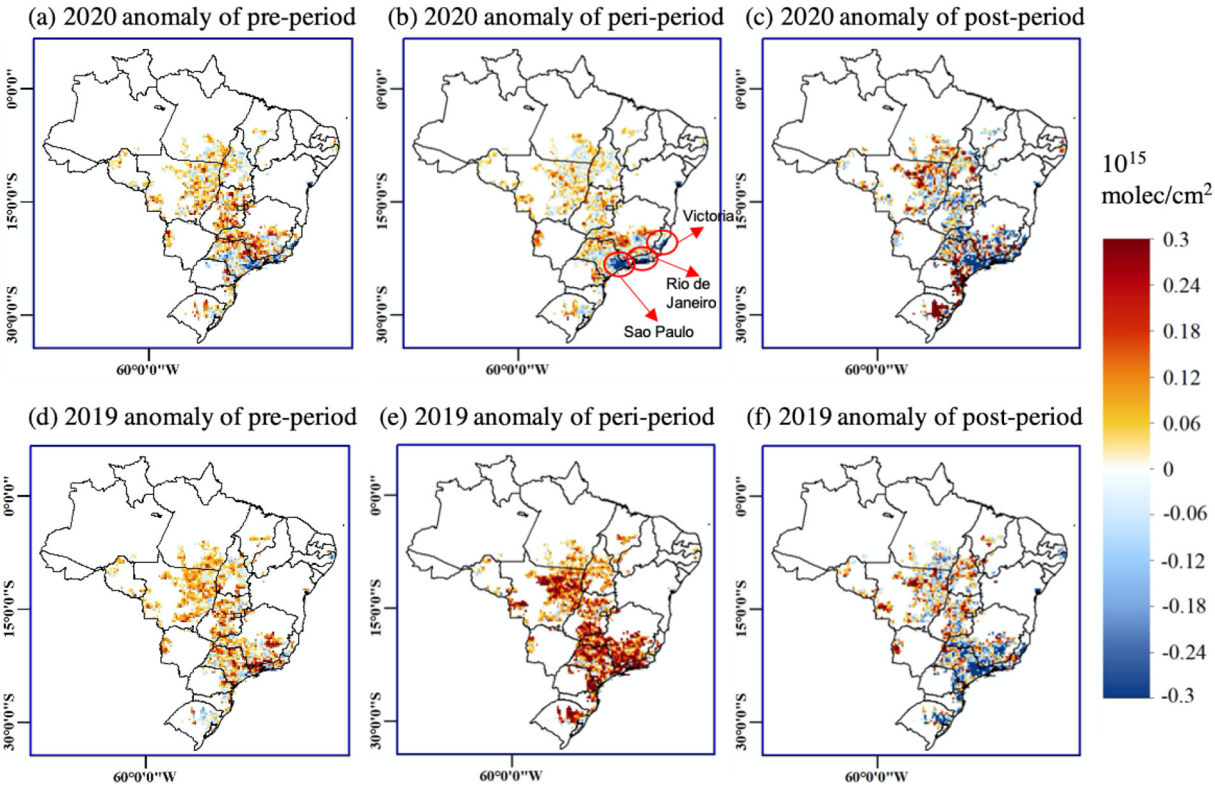

Fig. 8. Spatial patterns of NO_2 TVCD anomalies for pre-, peri- and post-period over Brazil. (a)–(c) anomalies for 2019; (d)–(f) anomalies for 2020. Pixels with annual means smaller than 1×10^{15} molec/cm^2 are not plotted in the maps.

However, similar phenomenon is observed in 2019 data. The overall increase is lower in 2020 and 2019 than 2010–2019 with RD of 27% and 23% versus 36%. Therefore, COVID-19 related shutdown and reopening orders do not have obvious influence on the overall NO_2 emissions of Brazil.

Fig. 8 shows spatial patterns of NO_2 TVCD anomalies for the pre-, peri- and post-period over Brazil. From the pre- to peri-period, despite the NO_2 columns increase over most target pixels in 2019, the 2020 data shows declines, especially over major cities like Rio de Janeiro, Vitoria and Sao Paulo. Lockdown-induced reduction of traffic emissions is the most likely reason for this phenomenon. Meanwhile, declines of NO_2 over rural areas are not significant considering the systematic errors and slightly lower initial emissions in the pre-period as compared with 2019. Therefore, the influence of COVID-19 on industrial production is not obvious in Brazil.

In the post-period, spatial patterns of NO_2 TVCDs are similar in the 2 years for most pixels and some of the southern parts such as Santa Maria city even has higher columns in 2020 than 2019, which indicates a rebound of the vehicle usage and traffic emissions after the shutdown order is lifted. Although the spatiotemporal average in this country does not show significant differences during the lockdown, the emissions in big cities are still thought to be highly influenced by the pandemic.

3.5. India

COVID-19 was first reported in India on January 30, 2020 (Ray, 2020). As the threat increased, the prime minister ordered a nationwide lockdown on March 24th (Withnall, 2020). As shown in Fig. 9, the 2020 trend of NO_2 TVCDs are consistent with both 2019 and 2010–2019 in the pre-period and even higher during February (days 43–67), possibly due to the high biomass burning, forest fires, vegetation, and agricultural crop emissions this year (Gautam et al., 2020). However, the 2020 data is generally below the curves of 2019 data and 10-year climatology in the peri-period. According to Table 2, the decline between the pre- and peri-period is 11% for 2020 data which is considerably sharper than 2019 and 2020 which are 1% and 3% respectively. Accordingly, the lockdown has significantly reduced the NO_2 emission in India indicating its negative impacts on the economy and people's activities. The unusual decline does not rebound to normal trends even after the reopening in 2020 with a RD between post- and pre-period of −11% compared to −3% for both 2019 and 2010–2019. In conclusion, economic production and transportation are impeded by the COVID-19 mitigation policies in India and have not recovered even after the lockdown orders are lifted.

As can be observed from the spatial patterns shown in Fig. 10, the majority of middle and northern India shows declines from the pre- to peri-period in 2020. These regions are populated cities and transportation

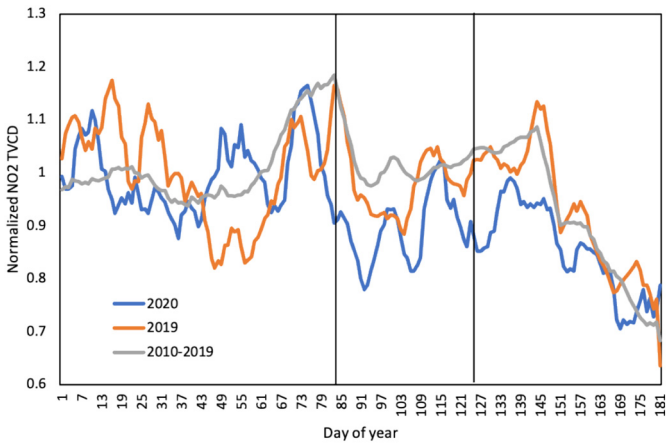

Fig. 9. Daily variations in 7-day moving averages of the NO_2 TVCD over India. The x-axis shows day-of-year. Points represent the midpoint of the 7-day interval. Values are normalized to the mean of the pre-period. The shadows represent standard errors. The two vertical lines divides the timeseries in to pre-, peri- and post-periods.

hubs such as Raj Nandgaon, Balaghat, Gadchiroli and Patnar, that are mainly located at the junctures of two states, near major power plants in India (World Resources Institute, 2019; Singh and Richmond, 2016; Fig. A.5). Compared to the increasing changes over these regions in 2019 for the same period, the decreasing patterns are most possibly due to the shutdown of transportation and industrial production in those cities.

Emissions bounce back in the western states, whereas decreases in some eastern regions, such as Dhanbad and Durgapur, are still significant compared to 2019. These regions are state borders with national highways and highly active transportations (NHAI, 2020), and due to the ongoing spread of COVID-19, traffic in these regions is still under great influence even after the lockdown is relieved.

3.6. United Kingdom

On January 31, 2020, UK's first case was confirmed (Wikipedia, 2020). COVID-19 mitigation policies, such as curfews and lockdowns, were issued in most regions in the country by March 23, 2020 (ITV News, 2020). As can be seen in Fig. 11, with an emission trend similar to the 2019 and historical data before the lockdown, the NO_2 time series falls lower than previous years during the peri-period in 2020, especially for the first 3–4 weeks. The decrease is extremely significant compared to 2019 (−34% vs −9%), reflecting negative impacts of COVID-19 on economic activities and NO_2 emissions. After industrial and city reopenings in 2020, the trend of NO_2 columns rebounds to a similar trend as compared with previous years. The average decline between the post- and pre-period is −54% compared to −46% and −55% for 2019 and 2010–2019 (Table 2), which is not significant considering the standard errors. The abnormal drop and uptick of NO_2 TVCD in 2020 of UK is coincident with the dates of COVID-19 lockdown and reopening orders, indicating their influences on economic productions and vehicle utilizations in the country.

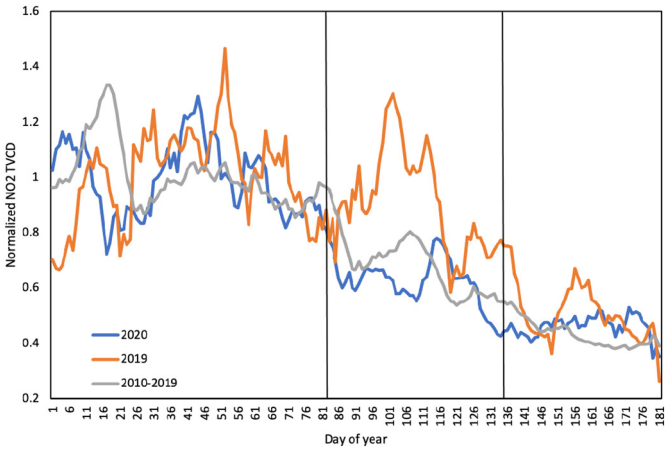

Fig. 11. Daily variations in 7-day moving averages of the NO_2 TVCD over the UK. The x-axis shows day-of-year. Points represent the midpoint of the 7-day interval. Values are normalized to the mean of the pre-period. These shadows represent standard errors. The two vertical lines divide the timeseries in to pre-, peri- and post-periods.

From the pre- to peri-period of 2020, the NO_2 columns show a decreasing change in central England (Fig. 12a, b), especially within the circled areas. The upper circle is concentrated with major coal-consumption power stations, such as Drax, Ratcliffe-on-Soar, Cottam and Ferrybridge (Global Energy Monitor, 2020). The lower circle locates the capital of the UK, London, surrounded by a number of power stations, such as Didcot and Beckenham. Most of these regions present increasing trends (Fig. 12d, e) during the same periods in 2019. The most possible explanation for these decreases is the shutdown of non-essential industries and the decline of transportations in cities. In small part, the closure of a few stations in these regions may also account for the reductions (UK Government, 2020). In the post-period of

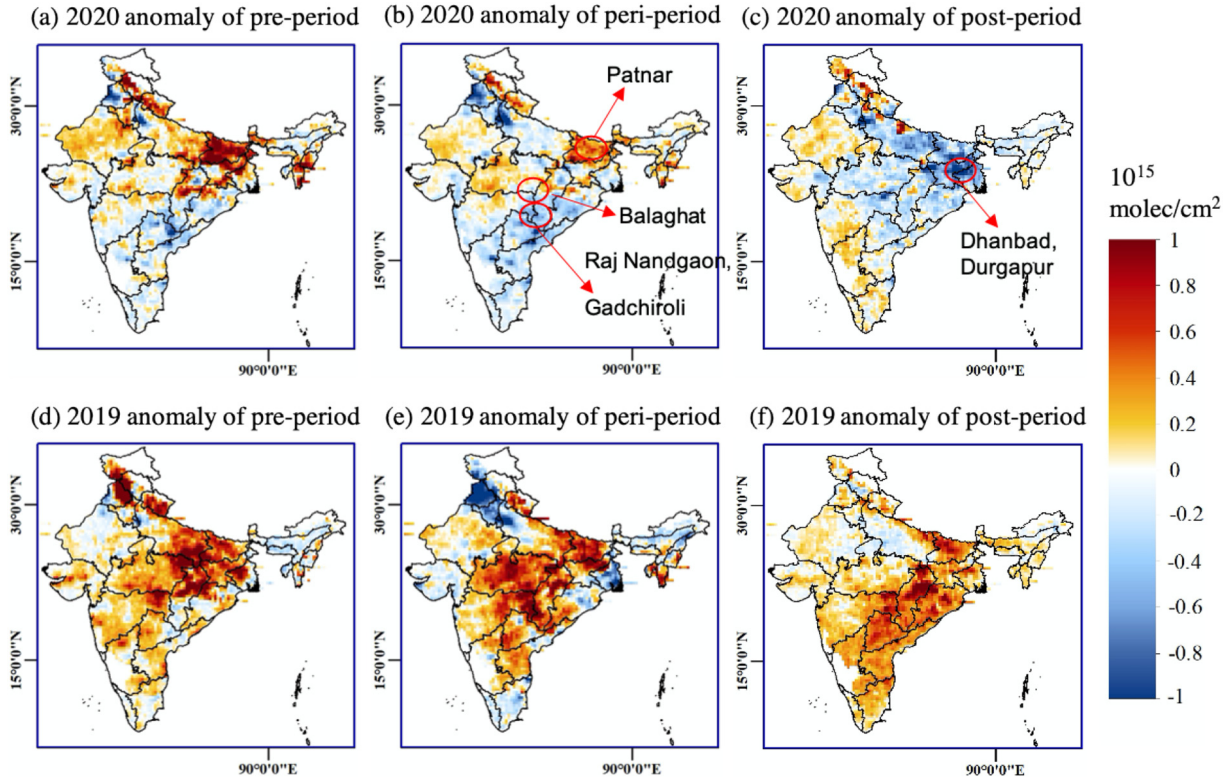

Fig. 10. Spatial patterns of NO_2 TVCD anomalies for the pre-, peri- and post-period over India. (a)–(c) anomalies for 2019; (d)–(f) anomalies for 2020. Pixels with annual means smaller than 1×10^{15} molec/cm^2 are not plotted in the maps.

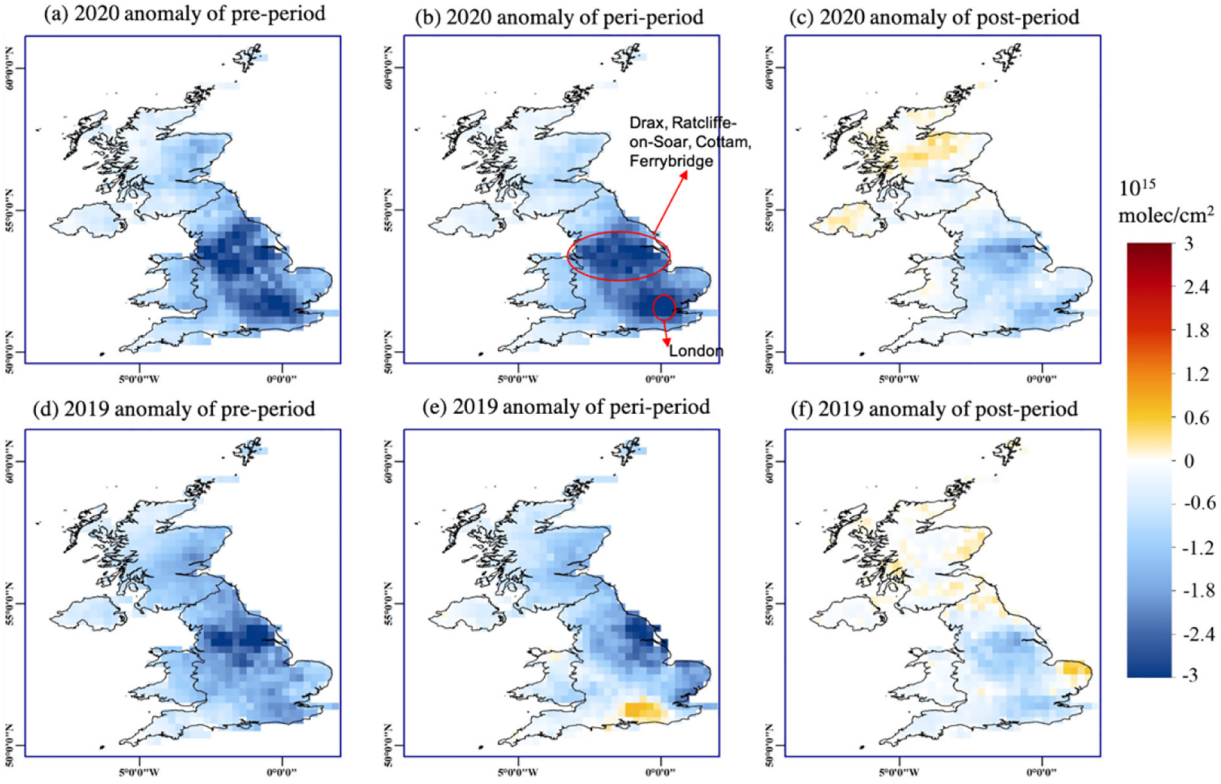

Fig. 12. Spatial patterns of NO_2 TVCD anomalies for pre-, peri- and post-period over the UK. (a)–(c) anomalies for 2019; (d)–(f) anomalies for 2020. Pixels with annual means smaller than 1×10^{15} molec/cm^2 are not plotted in the maps.

2020, the NO_2 columns show similar levels as 2019, indicating the rebound of the emissions thus the recovery of the economy.

4. Discussion

The paper analyzes the spatiotemporal patterns of NO_2 TVCDs before, during and after the pandemic triggered lockdown over different countries in 2020, comparing them with 2019 and the means of 2010–2019. We utilize relative differences, normalized timeseries, and spatial patterns of anomalies throughout the study to mitigate potential seasonal variations and data uncertainties which are not caused by COVID-19. To further rule out the inter-annual variations, the paper performs detrending analysis to exclude the linear trend between 2020 and 2019 in the three separate periods.

The economic lockdown and stay-at-home orders reduced the general NO_2 emissions in most study countries due to the shutdown of non-essential industries and reductions in transportation. After these policies were lifted, NO_2 emissions gradually rebounded to normal levels as work and industrial production resumed. However, despite similar overall trends in most study regions, the distributions of NO_2 patterns are dissimilar because of different geographical conditions (Naemura et al., 2001), varying travel and living habits, and local COVID-19 prevention policies. Brazil and the US did not present the decrease-and-uptick pattern as other countries on a national level. Nevertheless, regions of some populated cities, transportation hubs and major power plants follow this trend in these two countries. As a conclusion, lockdown and reopening orders due to COVID-19 influence the transportation and industrial production, thus the NO_2 emissions in all the study countries.

Fuel-burning from everyday domestic activities, such as the use of heaters and stoves, is an important source of NO_2 emissions in residential areas (Lee et al., 2002) (Kousa et al., 2001). It can be intuited that citizens spent more time staying in residential areas during the peri- period due to the stay-at-home orders and social distancing policies and would likely produce more NO_2 in their daily lives, which may also partially account for the patterns of NO_2 columns in some regions. On the other hand, meteorological variabilities and regulation measurements also influence the NO_2 columns in small part. These factors need to be analyzed separately using model simulations. Due to the data availability and study scope, they are not quantitatively calculated in this paper. Other explanations that may introduce errors are as follows:

1) The detrending analysis conducted by this paper only focuses on the linear trends, but the actual inter-annual signals in NO_2 emissions are more complex (Mahajan et al., 2015).
2) The selections of shutdown and reopening dates are estimations based on the policy stringencies of the overall condition for each target country. However, the actual starting point may vary for different regions in the same country, which may cause errors when calculating the RDs and changes.
3) The paper considers the seasonal variations and inter-annual trends during the study periods, however, factors such as wildfires, local transportations, climate and geographical changes may also contribute to the changes of patterns.
4) Errors from the raw NO_2 TVCD observations (Ionov et al., 2008).

Previous studies also illustrated changes in NO_2 emissions in different countries. Bauwens et al. (2020) reported reductions in NO_2 columns by up to 40% for the US regions and 40–60% in Chinese cities during the lockdown. Similarly, our study reveals a 41% decrease for the US and 53% decrease for China. Liu et al. (2020d) observed a 48% decline in NO_2 TVCD from the pre- to peri-period for entire China in 2020 compared to 53% from our study, which only focuses on the anthropogenic-dominated pixels. Despite the effort made by this study and all the other related research, more work needs to be done highlighting the various impacts of COVID-19 mitigation efforts, including:

1) Conducting detailed and quantitative analysis to explain spatiotemporal patterns at a regional or local scale, by considering more local features such as mitigation policies of counties/cities/states/

provinces, regional environment and weather, wildfires, residents' habits and customs, locations of roads and power/industrial plants, topography, etc.
2) Performing more comprehensive detrending analysis on the long-term historical data.
3) Including other potential parameters which may influence the patterns and trends of NO_2 emissions, such as human mobilities, inner-city transportation, climate and geographical changes, to isolate the influence of COVID-19 mitigation efforts more accurately;
4) Investigating the impacts of COVID-19 in other parts of the world.
5) Estimating the impacts of COVID-19 related policies on global economy.

5. Conclusions

Through the spatiotemporal patterns of NO_2 TVCD derived from the experiments and analysis, this paper concludes the following:

1) The COVID-19 lockdown and economic reopening policies have had crucial influences on the NO_2 emissions of most study countries in both spatial and temporal dimensions. These impacts are distinct in different countries in terms of duration, response speed, severeness of influence, and spatial distribution.
2) For the anthropogenic-sources-dominated pixels, mean NO_2 TVCDs of most target countries, including China, South Africa, India and UK, significantly decreased during the lockdown compared to 2019 and 2010–2019. However, the changes in RDs over Brazil and the US are relatively small and according to Bauwens et al. (2020), uncertainties of the OMNO2d product are larger than ±5% over most of their study cities during this period. Therefore, the overall NO_2 emissions have no obvious change in Brazil and the US. However, NO_2 columns were observed to be reduced over their metropolises, national capitals and power plants despite overall patterns, indicating the negative influence of COVID-19 on traffic volume and industrial production.
3) After the reopening, the NO_2 emissions rebounded to similar levels as the pre-period in most target countries except India. The NO_2 columns in India stay at a lower level compared to previous years, indicating that industrial production has not yet recovered from the pandemic.

CRediT authorship contribution statement

Qian Liu: Conceptualization, Investigation, Visualization, Writing – original draft. **Anusha Srirenganathan Malarvizhi:** Data curation. **Wei Liu:** Validation. **Hui Xu:** Formal analysis. **Jackson T. Harris:** Writing – review & editing. **Jingchao Yang:** Data curation. **Daniel Q. Duffy:** Conceptualization, Funding acquisition. **Michael M. Little:** Funding acquisition, Resources. **Dexuan Sha:** Data curation. **Hai Lan:** Project administration. **Chaowei Yang:** Conceptualization, Supervision, Writing – review & editing, Funding acquisition.

Declaration of competing interest

The authors declare that they have no known competing financial interests or personal relationships that could have appeared to influence the work reported in this paper.

Acknowledgements

The study is funded by NSF (1835507, 1841520 and 2027521) and NASA Center for Climate Simulations; OMI NO_2 data are from GES DISC: https://disc.gsfc.nasa.gov/datasets/OMNO2d_003/summary?keywords=omi.

References

Atkinson, R.W., Butland, B.K., Anderson, H.R., Maynard, R.L., 2018. Long-term concentrations of nitrogen dioxide and mortality: a meta-analysis of cohort studies. Epidemiology (Cambridge, Mass.) 29 (4), 460–472. https://doi.org/10.1097/EDE.0000000000000847.

Baldasano, J.M., 2020. COVID-19 lockdown effects on air quality by NO2 in the cities of Barcelona and Madrid (Spain). Sci. Total Environ. 741, 140353.

Bauwens, M., Compernolle, S., Stavrakou, T., Müller, J.F., Van Gent, J., Eskes, H., Levelt, P.F., van der A., R., Veefkind, J.P., Vlietinck, J., Yu, H., 2020. Impact of coronavirus outbreak on NO2 pollution assessed using TROPOMI and OMI observations. Geophys. Res. Lett. 47 (11) (p.e2020GL087978).

BBC News, 2020. Coronavirus: Brazil Reports Over 1,000 Deaths. https://www.bbc.com/news/world-latin-america-52251342 (August 5 2020).

Behera, S.N., Sharma, M., 2011. Degradation of SO_2, NO_2 and NH_3 leading to formation of secondary inorganic aerosols: an environmental chamber study. Atmos. Environ. 45 (24), 4015–4024.

Boren, Zach, 2015. China's Coal Bubble: 155 Coal-Fired Power Plants in the Pipeline Despite Overcapacity. https://unearthed.greenpeace.org/2015/11/11/chinas-coal-bubble-155-new-overcapacity/.

Brinksma, E.J., Pinardi, G., Volten, H., Braak, R., Richter, A., Schönhardt, A., Van Roozendael, M., Fayt, C., Hermans, C., Dirksen, R.J., Vlemmix, T., 2008. The 2005 and 2006 DANDELIONS NO2 and aerosol intercomparison campaigns. J. Geophys. Res.-Atmos. 113 (D16).

Businesstech, 2020. Ramaphosa announces 21-day coronavirus lockdown for South Africa. https://businesstech.co.za/news/government/383927/ramaphosa-announces-21-day-coronavirus-lockdown-for-south-africa/ (Access on July 25 2020).

Center for Disaster Philanthroy, 2020. 2020 North American Wildfire Season. https://disasterphilanthropy.org/disaster/2020-california-wildfires/ (Nov. 30 2020).

Charner, F., 2020. Brazil tops 1 million Covid-19 cases. It May Pass The US Next, Becoming The Worst-hit Country on the Planet. CNN https://www.cnn.com/2020/06/19/americas/brazil-one-million-coronavirus-jair-bolsonaro-cases-intl/index.html (Access on July 25 2020).

Crutzen, P.J., 1979. The role of NO and NO2 in the chemistry of the troposphere and stratosphere. Annu. Rev. Earth Planet. Sci. 7 (1), 443–472.

Dong, E., Du, H., Gardner, L., 2020. An interactive web-based dashboard to track COVID-19 in real time. The Lancet Infectious Diseases 20 (5), 533–534.

Duncan, B.N., Lamsal, L.N., Thompson, A.M., Yoshida, Y., Lu, Z., Streets, D.G., Hurwitz, M.M., Pickering, K.E., 2016. A space-based, high-resolution view of notable changes in urban NOx pollution around the world (2005–2014). J. Geophys. Res.-Atmos. 121 (2), 976–996.

Gautam, A.S., Dilwaliya, N.K., Srivastava, A., Kumar, S., Bauddh, K., Siingh, D., Shah, M.A., Singh, K., Gautam, S., 2020. Temporary reduction in air pollution due to anthropogenic activity switch-off during COVID-19 lockdown in northern parts of India. Environment, Development and Sustainability, pp. 1–24.

Global Energy Monitor, 2020. Global Coal Plant Tracker. https://endcoal.org/tracker/ (Dec. 2 2020).

Hale, T., Petherick, A., Phillips, T., Webster, S., 2020. Variation in government responses to COVID-19. Blavatnik school of government working paper, 31, p. 2020-11.

Ionov, D.V., Timofeyev, Y.M., Sinyakov, V.P., Semenov, V.K., Goutail, F., Pommereau, J.P., Bucsela, E.J., Celarier, E.A., Kroon, M., 2008. Ground-based validation of EOS-Aura OMI NO2 vertical column data in the midlatitude mountain ranges of Tien Shan (Kyrgyzstan) and Alps (France). J. Geophys. Res.-Atmos. 113 (D15).

ITV News, 2020. Boris Johnson Orders Three-Week Lockdown of UK to Tackle Coronavirus Spread. https://www.itv.com/news/2020-03-23/boris-johnson-downing-street-coronavirus-update (Retrieved 23 March 2020).

Jie, Z.H.A.N.G., Ang, L.I., Pin-Hua, X.I.E., Feng-Cheng, W.U., Jin, X.U., Jin-Chao, S.H.E.N., Zheng, R.E.N.G., Fu-Sheng, M.O.U., Zhao-Kun, H.U., 2016. Spatiotemporal variation characteristics of NO_2 tropsopheric column concentration over Chinese Central region based on OMI data during 2007–2014. J. Atmos. Environ. Opt. 11 (4), 288.

Judeikis, H.S., Wren, A.G., 1978. Laboratory measurements of NO and NO_2 depositions onto soil and cement surfaces. Atmospheric Environment (1967) 12 (12), 2315–2319.

Kousa, A., Monn, C., Rotko, T., Alm, S., Oglesby, L., Jantunen, M.J., 2001. Personal exposures to NO2 in the EXPOLIS-study: relation to residential indoor, outdoor and workplace concentrations in Basel, Helsinki and Prague. Atmos. Environ. 35 (20), 3405–3412.

Krotkov, N.A., McLinden, C.A., Li, C., Lamsal, L.N., Celarier, E.A., Marchenko, S.V., Swartz, W.H., Bucsela, E.J., Joiner, J., Duncan, B.N., Boersma, K.F., 2016. Aura OMI observations of regional SO 2 and NO 2 pollution changes from 2005 to 2015. Atmos. Chem. Phys. 16 (7), 4605.

Lee, H.J., Koutrakis, P., 2014. Daily ambient NO_2 concentration predictions using satellite ozone monitoring instrument NO_2 data and land use regression. Environ. Sci. Technol. 48 (4), 2305–2311.

Lee, K., Xue, J., Geyh, A.S., Ozkaynak, H., Leaderer, B.P., Weschler, C.J., Spengler, J.D., 2002. Nitrous acid, nitrogen dioxide, and ozone concentrations in residential environments. Environ. Health Perspect. 110 (2), 145–150.

Li, J., Wang, Y., 2019. Inferring the anthropogenic NO x emission trend over the United States during 2003–2017 from satellite observations: was there a flattening of the emission trend after the Great Recession? Atmos. Chem. Phys. 19 (24), 15339–15352.

Liu, F., Page, A., Strode, S.A., Yoshida, Y., Choi, S., Zheng, B., Lamsal, L.N., Li, C., Krotkov, N.A., Eskes, H., Veefkind, P., 2020d. Abrupt decline in tropospheric nitrogen dioxide over China after the outbreak of COVID-19. Sci. Adv. 6 (28), 1–5.

Liu, Q., Sha, D., Liu, W., Houser, P., Zhang, L., Hou, R., Lan, H., Flynn, C., Lu, M., Hu, T., Yang, C., 2020a. Spatiotemporal patterns of COVID-19 impact on human activities and environment in mainland China using nighttime light and air quality data. Remote Sens. 12 (10), 1576.

Liu, Q., Liu, W., Sha, D., Kumar, S., Chang, E., Arora, V., Lan, H., Li, Y., Wang, Z., Zhang, Y., Zhang, Z., 2020b. An environmental data collection for COVID-19 pandemic research. Data 5 (3), 68.

Liu, Q., Harris, J.T., Chiu, L.S., Sun, D., Houser, P.R., Yu, M., Duffy, D.Q., Little, M.M., Yang, C., 2020c. Spatiotemporal impacts of COVID-19 on air pollution in California, USA. Science of The Total Environment, p. 141592.
Mahajan, A.S., De Smedt, I., Biswas, M.S., Ghude, S., Fadnavis, S., Roy, C., van Roozendael, M., 2015. Inter-annual variations in satellite observations of nitrogen dioxide and formaldehyde over India. Atmos. Environ. 116, 194–201.
McMichael, et al., 2020. COVID-19 in a Long-Term Care Facility — King County, Washington, February 27–March 9, 2020. https://www.cdc.gov/mmwr/volumes/69/wr/mm6912e1.htm Access on July 25 2020.
Ministerio da Saude, 2020. Brasil confirma primeiro caso da doença. https://www.saude.gov.br/noticias/agencia-saude/46435-brasil-confirma-primeiro-caso-de-novo-coronavirus (Access on July 25 2020).
Moon, Sarah, April 24, 2020. A seemingly healthy woman's sudden death is now the first known US coronavirus-related fatality. CNN (Retrieved May 25, 2020).
Naemura, A., Tsuchiya, A., Nakane, K., 2001. Climatological and geographical characteristics within inversion layers in the presence of high NO 2 concentration. Water Air Soil Pollut. 130 (1–4), 343–348.
National Highways Authority of India, 2020. State wise distribution of National Highways. https://web.archive.org/web/20130215043627/https://www.nhai.org/statewise1.asp (Access on Dec. 2 2020).
Norwood, C., 2020. Most states have issued stay-at-home orders, but enforcement varies widely. PBS https://www.pbs.org/newshour/politics/most-states-have-issued-stay-at-home-orders-but-enforcement-varies-widely (Access on July 25 2020).
Ogen, Y., 2020. Assessing Nitrogen Dioxide (NO_2) Levels as a Contributing Factor to the Coronavirus (COVID-19) Fatality Rate. Science of The Total Environment, p. 138605.
Otmani, A., Benchrif, A., Tahri, M., Bounakhla, M., El Bouch, M., Krombi, M.H., 2020. Impact of Covid-19 lockdown on PM10, SO2 and NO2 concentrations in Salé City (Morocco). Science of The Total Environment, p. 139541.
Pollet, B.G., Staffell, I., Adamson, K.A., 2015. Current Energy Landscape in the Republic of South Africa. Int. J. Hydrog. Energy 40 (46), 16685–16701.
Ray, M., 2020. India Most Infected by Covid-19 among Asian Countries, Leaves Turkey Behind. Hindustan Times https://www.hindustantimes.com/india-news/india-most-infected-by-covid-19-among-asian-countries-leaves-turkey-behind/story-Jjd0AqIsuL3yjMWg29uJ3I.html (Access on July 25 2020).
Richter, A., Burrows, J.P., Nüß, H., Granier, C., Niemeier, U., 2005. Increase in tropospheric nitrogen dioxide over China observed from space. Nature 437 (7055), 129–132.
Riechmann, D., 2020. US Declares Public Health Emergency From Coronavirus. Boston Globe https://www.bostonglobe.com/news/nation/2020/01/31/declares-public-health-emergency-from-coronavirus/9WMXL38AdA08GJworROtII/story.html (Access on July 25 2020).
Shou, M.H., Wang, Z.X., Li, D.D., Wang, Y., 2020. Assessment of the air pollution emission reduction effect of the coal substitution policy in China: an improved grey modelling approach. Environ. Sci. Pollut. Res. 27 (27), 34357–34368.
Singh, K., Richmond, J., 2016. A Win for India is a Win for the World: Why the United States Needs to Help India Clean up Its Coal. https://www.cgdev.org/blog/win-india-win-world-why-united-states-needs-help-india-clean-its-coal (Access on Dec. 2 2020).
South African Government, 2020a. Minister Zweli Mkhize reports first case of Coronavirus Covid-19. https://www.gov.za/speeches/health-reports-first-case-covid-19-coronavirus-5-mar-2020-0000 (Access on July 25 2020).
South African Government, 2020b. Travel - Coronavirus COVID-19. https://www.gov.za/Coronavirus/travel (Access on July 25 2020).
The Government of the Kingdom of Eswatini, 2020. National Response to COVID19 Updates by Government of the Kingdom of Eswatini. http://www.gov.sz/index.php/covid-19-corona-virus/situational-analysis (Access on July 25 2020).
UK Government, 2020. National Statistics: Digest of UK Energy Statistics (DUKES): Electricity. https://www.gov.uk/government/statistics/electricity-chapter-5-digest-of-united-kingdom-energy-statistics-dukes (Access on Dec. 2 2020).
Villena, G., Bejan, I., Kurtenbach, R., Wiesen, P., Kleffmann, J., 2012. Interferences of commercial NO_2 instruments in the urban atmosphere and in a smog chamber. Atmospheric Measurement Techniques 5 (1), 149.
Wikipedia, 2020. COVID-19 pandemic in the United Kingdom. https://en.wikipedia.org/wiki/COVID-19_pandemic_in_the_United_Kingdom (Access on Dec. 2 2020).
Withnall, A., 2020. India Coronavirus: Modi Announces 21-day Nationwide Lockdown, Limiting Movement of 1.4bn People. Independent https://www.independent.co.uk/news/world/asia/india-coronavirus-lockdown-modi-speech-cases-update-news-a9421491.html (Access on July 25 2020).
World Resources Institute, 2019. Global Power Plant Database. https://datasets.wri.org/dataset/globalpowerplantdatabase (Access on May 10 2020).
Yang, C., Sha, D., Liu, Q., Li, Y., Lan, H., Guan, W.W., Hu, T., Li, Z., Zhang, Z., Thompson, J.H., Wang, Z., 2020. Taking the pulse of COVID-19: a spatiotemporal perspective. International Journal of Digital Earth 1–26.
Zambrano-Monserrate, M.A., Ruano, M.A., Sanchez-Alcalde, L., 2020. Indirect Effects of COVID-19 on the Environment. Science of the Total Environment, p. 138813.
Zhu, Y., Xie, J., Huang, F., Cao, L., 2020. Association between short-term exposure to air pollution and COVID-19 infection: Evidence from China. Sci. Total Environ. 138704.
Zu, Z.Y., Jiang, M.D., Xu, P.P., Chen, W., Ni, Q.Q., Lu, G.M., Zhang, L.J., 2020. Coronavirus disease 2019 (COVID-19): a perspective from China. Radiology, p. 200490.